Identification of the 4-Glutamyl Radical as an Intermediate in the Carbon Skeleton Rearrangement Catalyzed by Coenzyme B_{12}-Dependent Glutamate Mutase from *Clostridium cochlearium*†

Harald Bothe,‡ Daniel J. Darley,§ Simon P. J. Albracht,|| Gary J. Gerfen,⊥ Bernard T. Golding,§ and Wolfgang Buckel*,‡

Laboratorium für Mikrobiologie, Fachbereich Biologie, Philipps-Universität, D-35032 Marburg, Germany, Francis Bitter Magnet Laboratory, Department of Chemistry, Massachusetts Institute of Technology, Cambridge, Massachusetts 02139, Department of Chemistry, Bedson Building, University of Newcastle upon Tyne, Newcastle upon Tyne NE1 7RU, United Kingdom, and E. C. Slater Institute, BioCentrum Amsterdam, Plantage Muidergracht 12, NL-1018 TV Amsterdam, The Netherlands

Received June 11, 1997; Revised Manuscript Received January 12, 1998

ABSTRACT: A series of ^{2}H- and ^{13}C-labeled glutamates were used as substrates for coenzyme B_{12}-dependent glutamate mutase, which equilibrates (*S*)-glutamate with (2*S*,3*S*)-3-methylaspartate. These compounds contained the isotopes at C-2, C-3, or C-4 of the carbon chain: [2-^{2}H], [3,3-$^2H_2$], [4,4-$^2H_2$], [2,3,3,4,4-$^2H_5$], [2-^{13}C], [3-^{13}C], and [4-^{13}C]glutamate. Each reaction was monitored by electron paramagnetic resonance (EPR) spectroscopy and revealed a similar signal characterized by $g'_{xy} = 2.1$, $g'_z = 1.985$, and $A' = 5.0$ mT. The interpretation of the spectral data was aided by simulations which gave close agreement with experiment. This approach underpinned the idea of the formation of a radical pair, consisting of cob(II)alamin interacting with an organic radical at a distance of 6.6 ± 0.9 Å. Comparison of the hyperfine couplings observed with unlabeled glutamate with those from the labeled glutamates enabled a principal contributor to the radical pair to be identified as the 4-glutamyl radical. These findings support the currently accepted mechanism for the glutamate mutase reaction, i.e., the process is initiated through hydrogen atom abstraction from C-4 of glutamate by the 5′-deoxyadenosyl radical, which is derived by homolysis of the Co−C σ-bond of coenzyme B_{12}.

Coenzyme B_{12}-dependent glutamate mutase catalyzes the reversible carbon skeleton rearrangement of (*S*)-glutamate (**1a**) to (2*S*,3*S*)-3-methylaspartate (**2a**) (Scheme 1) [for reviews see Switzer (1982) and Buckel and Golding (1996)]. This is the first step in the fermentation of glutamate to acetate and butyrate in many clostridia such as *Clostridium tetani*, *Clostridium tetanomorphum*, and *Clostridium cochlearium* (Buckel & Barker, 1974; Buckel, 1980). The enzyme from *C. cochlearium* consists of two protein components: E, a homodimer (ϵ_2, 2 × 53.5 kDa) and S, a monomer (σ, 14.8 kDa; Leutbecher et al., 1992). Both components can be overproduced separately in *Escherichia coli* (Zelder et al., 1994a,b). Incubation of the purified recombinant components E and 2 S with coenzyme B_{12} (5′-deoxyadenosylcobalamin) results in the formation of an active holoenzyme ($\epsilon_2\sigma_2$) containing one molecule of the coenzyme.

Scheme 1: Proposed Reversible Fragmentation of the 4-Glutamyl Radical (**3a**) into Glycinyl Radical (**5a**) and Acrylate (**6**) Followed by Recombination to 3-Methyleneaspartate Radical (**4a**)

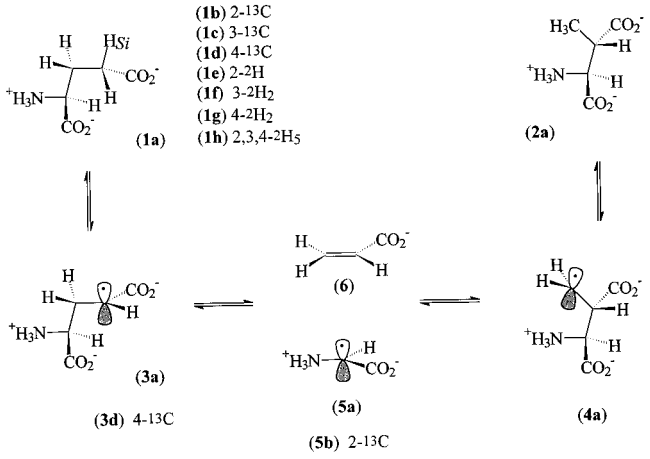

It is generally accepted that coenzyme B_{12}-dependent rearrangements are initiated by homolytic cleavage of the cobalt−carbon σ-bond of coenzyme B_{12}, which affords the 5′-deoxyadenosyl radical and cob(II)alamin. The 5′-deoxyadenosyl radical abstracts a hydrogen atom from a substrate molecule to generate a substrate-derived radical. This rearranges to a product-related radical that retrieves a

† Dedicated to Professor Hermann Eggerer on the occasion of his 70th birthday. This work was supported by grants from the European Commission, Deutsche Forschungsgemeinschaft, Fonds der Chemischen Industrie, Engineering and Physical Sciences Research Council, and by National Institutes of Health Grants GM-29595, GM-38352, and RR-00995

* Author to whom correspondence should be addressed.
‡ Philipps-Universität.
§ University of Newcastle upon Tyne.
|| E. C. Slater Institute.
⊥ Massachusetts Institute of Technology. Present address: Department of Physiology and Biophysics, Albert Einstein College of Medicine, 1300 Morris Park Ave., Bronx, NY 10461.

S0006-2960(97)01393-7 CCC: $15.00
Published on Web 03/05/1998

hydrogen atom from the methyl group of 5′-deoxyadenosine, giving the product and regenerating the 5′-deoxyadenosyl radical, which can initiate a new reaction cycle (Abeles & Dolphin, 1976; Golding, 1982).

During the glutamate mutase reaction, a glycinyl residue is transferred *intra*molecularly from C-3 to C-4 of the (*S*)-glutamate carbon skeleton. In parallel, a hydrogen atom migrates *inter*molecularly via 5'-deoxyadenosine from C-4 to C-3. It is postulated that H abstraction from the C-4 position of (*S*)-glutamate (**1a**, Scheme 1) generates the 4-glutamyl radical (**3a**), which is converted into a radical (**4a**) related to 3-methylaspartate (**2a**) (Scheme 1). It has also been proposed that the 4-glutamyl radical (**3a**) fragments into a 2-glycinyl radical (**5a**) and acrylate (**6**), which can recombine either to re-form radical **3a** or to give the product-related radical (**4a**) (Beatrix et al., 1995; Buckel & Golding, 1996). Donation of a hydrogen atom from 5′-deoxyadenosine to radical (**3a**) regenerates (*S*)-glutamate (**1a**), while donation of H to (**4a**) gives (2*S*,3*S*)-3-methylaspartate (**2a**). In the simplest form of this mechanism, there is no role for cob(II)alamin, which merely acts as a spectator or voyeur (Golding & Radom, 1976; Rétey, 1982; Babior, 1988). None of the radicals proposed as intermediates has been characterized.

Cob(II)alamin and the 5′-deoxyadenosyl radical produced by homolysis of the cobalt−carbon bond of coenzyme B_{12} are expected to give an electron paramagnetic resonance (EPR)[1] spectrum with $g_{xy} = 2.25$ and $g_z = 2.004$ for cob(II)alamin and $g_{xyz} \sim 2.0$ for the 5′-deoxyadenosyl radical. The g_z signal of cob(II)alamin shows an 8-fold hyperfine splitting due to the interaction of the free electron ($S = {}^1/_2$) with the nuclear spin of Co ($I = {}^7/_2$) with a hyperfine splitting constant $A' = 1.1$ mT (Pilbrow, 1982). In addition there is superhyperfine splitting of the 8 g_z lines, which is caused by the coordination of an axial ^{14}N ligand ($I = 1$) from a conserved histidine of the protein to the cobalt (Stupperich et al., 1990; Luschinsky Drennan et al., 1994; Zelder et al., 1995; Padmakumar et al., 1995). However, EPR measurements performed with the enzymatically active protein components, coenzyme B_{12}, and (*S*)-glutamate displayed only one EPR signal with lower *g* values than expected (Leutbecher et al., 1992). The EPR signal observed ($g'_{xy} \approx 2.1$, $g'_z = 1.985$, $A' = 5.0$ mT) was interpreted to be that of a biradical generated by the interaction of cob(II)alamin with an organic radical and it was shown to relate to a catalytically active state (Zelder et al., 1994a). The superhyperfine coupling of the g_z line of cob(II)alamin was unresolved, probably due to the influence of the additional radical species.

The EPR spectra from catalytically active glutamate mutase show similarities to the substrate-induced signals observed with the carbon skeleton rearranging enzymes 2-methyleneglutarate mutase (Michel et al., 1992; Zelder & Buckel, 1993; Beatrix et al., 1995) and methylmalonyl-CoA mutase (Zhao et al., 1992, 1994; Padmakumar & Banerjee, 1995). All of the spectra resemble the spectrum reported for the rapid reaction intermediate found in adenosylcobalamin-dependent ribonucleotide triphosphate reductase from *Lactobacillus leichmannii* (Orme-Johnson et al., 1974). The EPR spectrum from this ribonucleotide reductase was recently interpreted as representing a protein-based thiyl radical coupled to cob(II)alamin at a distance of ca. 6 Å (Licht et al., 1996; Gerfen et al., 1996).

On incubating glutamate mutase with (*S*)-[2,3,3,4,4-$^2H_5$]-glutamate (perdeuterated glutamate, **1h**), an EPR signal was observed with lower intensity and narrowed features compared to the signal derived from unlabeled glutamate (Zelder et al., 1994a). Substitution of a proton by deuterium reduces the hyperfine coupling by a factor proportional to the nuclear gyromagnetic ratio γ ($\gamma_D/\gamma_H = 0.153$) and therefore causes narrowing of EPR spectral features (Wertz & Bolton, 1986). On the basis of these observations it was suggested that a glutamate-derived radical participates in the glutamate mutase reaction (Zelder et al., 1994a). To identify this radical we have performed EPR experiments with glutamate mutase and all possible regiospecifically ^2H- and ^{13}C-labeled glutamates (**1b**−**1h**). In contrast to the effect of ^2H substitution on an EPR spectrum, ^{13}C substitution at a radical center causes broadening of the signals. This paper details the results and interpretation of our studies.

MATERIALS AND METHODS

Expression of glmS and glmE. *Escherichia coli* strain MC 4100 containing the expression vector pOZ3 (Zelder et al., 1994b) and *E. coli* strain DH5α containing pOZ5 (Zelder et al., 1994a) were used for overproduction of glutamate mutase components S and E, respectively. The bacteria were grown to $OD_{578} \approx 1$ on Standard 1 nutrient broth (Merck, Darmstadt, Germany) followed by addition of 1 mM isopropyl 1-thio-β-D-galactoside. After a further 15 h the bacteria were harvested by centrifugation.

Purification of Components E and S. Enzyme activity was measured using the spectrophotometric assay developed by Barker et al. (1964). For purification of recombinant component E, the harvested *E. coli* cells were resuspended in buffer A (20 mM potassium phosphate, pH 7.4, and 1 mM EDTA) and sonicated for 10 min followed by ultracentrifugation at 100000*g* for 30 min. The supernatant was applied to a phenyl-Sepharose column (HiLoad 26/10, Pharmacia) previously equilibrated with buffer B (buffer A containing 1 M ammonium sulfate). A decreasing linear ammonium sulfate gradient (buffer B to buffer A, 160 mL) was used to remove *E. coli* proteins. Component E was eluted with water and concentrated to less than 10 mL by using an Amicon chamber with a YM 30 filter membrane. The concentrate was applied to a Superdex 200 column (Pharmacia) and eluted with buffer A. Recombinant component S was purified as described for component E, with the exception that component S was eluted at ca. 0.2 M ammonium sulfate from the phenyl-Sepharose column (ammonium sulfate gradient: buffer B to 80% buffer A, 100 mL, followed to 100% buffer A, 300 mL). To buffers A and B, 2 mM dithiothreitol was added and removed by dialysis after each column run. The purification procedures were monitored by SDS−PAGE. For EPR experiments, components E and S were concentrated to 100 mg of protein/mL by using Centricon 30 and Centricon 10, respectively.

[1] Abbreviations: CoA, coenzyme A; EDTA, ethylenediaminetetraacetic acid; ENDOR, electron nuclear double resonance; EPR, electron paramagnetic resonance; ESEEM, electron spin−echo envelope modulation; K_{eq}, equilibrium constant; K_m, Michaelis constant; NAD^+, nicotinamide adenine dinucleotide; nkat, nanomoles per second (enzymatic activity); NMR, nuclear magnetic resonance; SDS−PAGE, sodium dodecyl sulfate−polyacrylamide gel electrophoresis; V_{max}, maximal velocity.

^{2}H-Labeled Glutamates. (*S*)-[2-^{2}H]Glutamate (**1e**) was synthesized by incubating 25 mM deuterioformate (Cambridge Isotope Laboratories), 2 mM NAD^+, 15 mM 2-oxoglutarate, and 7.5 mM ammonium sulfate with 85 nkat of formate dehydrogenase (Boehringer Mannheim) and 2000 nkat of glutamate dehydrogenase (Boehringer Mannheim) in 0.1 M potassium phosphate buffer, pH 7.4, at 37 °C for 7 days. In this system, deuterium was transferred from formate to 2-oxoglutarate via NAD^+. The deuterated glutamate species was absorbed on Dowex 50W × 8, H^+ form, and eluted with 1.5 M ammonia. The labeling, which was near-total isotopic exchange at C-2, was confirmed by ^{1}H NMR (300 MHz, D_2O): δ (ppm) 2.2 (m, 2 H, 2H-3), 2.4 (t, 2 H, 2H-4).

(*S*)-[3,3-$^2H_2$]Glutamate (**1f**) was synthesized by incubating 10 mM 2-oxo[3,3-$^2H_2$]glutarate with 1000 nkat of glutamate dehydrogenase, 7.5 mM ammonium sulfate, and 0.2 mM NADH in 0.1 M potassium phosphate buffer, pH 7, at 37 °C for 7 days. For NADH regeneration, 15 mM formate and 42 nkat of formate dehydrogenase were added. 2-Oxo-[3,3-$^2H_2$]glutarate was generated by heating 0.5 M 2-oxoglutarate in D_2O for 20 min at 120 °C (Rose, 1960; Hartrampf & Buckel, 1984). The (*S*)-glutamate was purified as above and ^{1}H NMR indicated almost total isotopic exchange at C-3 (300 MHz, D_2O): δ (ppm) 2.4 (br s, 2 H, 2H-4), 3.8 (br s, 1 H, H-2).

For the synthesis of [4,4-$^2H_2$]glutamate (**1g**), (*S*)-glutamate was dissolved in D_2O and freeze-dried. The residue was taken up in 6 M DCl to a solution 1 M in glutamate that was refluxed for 5 days (Murray & Williams, 1958). Removal of the excess of deuterated hydrochloric acid gave **1g**, which showed by ^{1}H NMR 90% deuteration of [4,4-$^2H_2$]-glutamate (i.e., ≈80% [4,4-$^2H_2$]glutamate + 20% [4-^{2}H]-glutamate): δ (ppm) 2.2 (m, 2 H, 2H-3), 2.6 (quartet, residual H-4), 4.1 (t, 1 H, H-2). Perdeuterated glutamate (**1h**) was from Cambridge Isotope Laboratories. The three regiospecific deuterated glutamate species were used as substrates for the determination of kinetic isotope effects in the spectrophotometric assay.

^{13}C-Labeled Glutamates. *rac*-[2-^{13}C]Glutamic acid (**1b**) and *rac*-[3-^{13}C]glutamic acid (**1c**) were purchased from Campro Scientific, Emmerich, Germany. (*S*)-[4-^{13}C]Glutamate (**1d**) was synthesized from diethyl [2-^{13}C]malonate. Thus, condensation of the sodium salt of diethyl [2-^{13}C]malonate (Cambridge Isotope Laboratories) with ethyl 2-(bromomethyl)acrylate (Villieras & Rambaud, 1982) in ethanol at 0 °C gave diethyl 4-ethoxycarbonyl-2-methylene[4-^{13}C]glutarate, which was ozonized in methanol at −78 °C to afford diethyl 4-ethoxycarbonyl-2-oxo[4-^{13}C]glutarate. Hydrolysis of this triester in 1 M hydrochloric acid at 100 °C and concomitant selective monodecarboxylation of the resulting triacid gave 2-oxo[4-^{13}C]glutarate, which was converted into (*S*)-[4-^{13}C]glutamate in the manner described above for deuterated glutamate. ^{1}H NMR (300 MHz, D_2O): δ (ppm) 2.2 (m, 2 H, 2H-3), 2.6 (dt, J = 128 Hz, 2 H, 2H-4), 4.0 (m, 1 H, H-2). ^{13}C NMR (300 MHz, D_2O): δ (ppm) 40.3.

^{15}N-Labeled glutamate was synthesized by incubating 15 mM 2-oxoglutarate, 15 mM $^{15}NH_4Cl$ (Cambridge Isotope Laboratories), 2 mM NAD^+, and 15 mM sodium formate with 85 nkat of formate dehydrogenase and 2000 nkat of glutamate dehydrogenase in 0.1 M potassium phosphate buffer, pH 7.4, at 37 °C for 7 days. [^{15}N]Glutamate was purified as described above. ^{1}H NMR (300 MHz, D_2O): δ (ppm) 2.1 (m, 2 H, 2H-3), 2.3 (m, 2 H, 2H-4), 3.8 (quartet, 1 H, H-2). ^{15}N NMR (50 MHz, DMSO-d_6): δ (ppm) = −341.8, referenced to the external standard nitromethane.

EPR Spectroscopy. Spectra were recorded with a Bruker ECS-106 EPR spectrometer at a temperature of 50 K, 9.4 GHz microwave power, 100 kHz modulation frequency, 0.63 mT modulation amplitude. For some control experiments at 77 K a Varian E-3 spectrometer was used (9.105 GHz microwave power, 100 kHz modulation frequency, 0.5 mT modulation amplitude). Component E (0.40−0.69 mM), component S (0.67−1.35 mM), and 1.6 mM coenzyme B_{12} were preincubated for 5 min with 10 mM 2-mercaptoethanol at ambient temperature in 20 mM Tris-HCl, pH 8.3. The reaction was started with 30 mM substrate to give a total volume of 0.3 mL. After incubation for ca. 20 s at room temperature, during which time complete equilibration between (*S*)-glutamate and (2*S*,3*S*)-3-methylaspartate was reached as indicated by the turnover number of component E (13 s^{-1}, see also Results), the reaction was stopped by freezing in liquid nitrogen. All experiments were carried out in the dark or under a red light. When D_2O was the solvent, H_2O was removed from components E and S by repeated concentration of the protein fractions in Centricon 10 tubes following addition of D_2O. Coenzyme B_{12}, glutamate, Tris-HCl, and 2-mercaptoethanol were prepared in D_2O in the same concentrations as those given above.

Simulation of EPR Spectra. The procedure used to simulate the EPR spectra has been previously described (Gerfen et al., 1996). Briefly, an electronic Hamiltonian incorporating the anisotropic Zeeman interaction for each electron spin species, as well as an isotropic exchange coupling and anisotropic dipolar coupling (zero-field splitting interaction) between the electron spins, is diagonalized to obtain electron spin state energies and associated eigenvectors. These eigenvectors are used to determine EPR transition probabilities and to calculate the expectation value of the electron spin for each state. The expectation value of each electron spin is used to determine the hyperfine field experienced by that electron from nuclei coupled to it through anisotropic hyperfine interactions (presently, the simulation program allows two nuclei to be coupled to each electron spin). The hyperfine interaction energies are then combined with electron spin state energies. A full frequency domain powder pattern calculation is performed at each magnetic field strength sampled (typically 375 positions across the simulated spectrum). The probabilities of those transitions, whose resonance frequencies lie within typically 3 MHz of the EPR frequency, are "binned" at that particular field sample.

The overall simulation strategy and parameter selection procedure was as follows. Hamiltonian parameters (principal values and orientations) for the cob(II)alamin species (Zeeman interaction, cobalt hyperfine interaction, nitrogen hyperfine interaction) were taken to be in the range previously determined for free cob(II)alamin (Pilbrow, 1982). Parameters that were varied to achieve the fits include the electron−electron exchange and dipolar interactions, the organic radical Zeeman and hyperfine interactions, and the relative orientations of the two species. Precise uncertainties are difficult to assign without a more extensive least-squares fitting routine and treatment of parameter correlation, which is

Table 1: Parameters Used in the Simulations of the EPR Spectra

	principal values	direction cosines		
g (cobalamin)	2.230	1.000	0.000	0.000
	2.235	0.000	1.000	0.000
	2.009	0.000	0.000	1.000
g (radical)	2.0043	1.000	0.000	0.000
	2.0037	0.000	1.000	0.000
	2.0021	0.000	0.000	1.000
$\mathbf{A}^{Co}$ (MHz)	15	0.643	0.766	0.000
	36	−0.766	0.643	0.000
	310	0.000	0.000	1.000
$\mathbf{A}^{N}$ (MHz)	35	1.000	0.000	0.000
	50	0.000	1.000	0.000
	50	0.000	0.000	1.000
D (MHz)	−50	0.985	0.000	−0.174
	−150	0.133	0.643	0.754
	200	0.112	−0.766	0.633
J_{ex} (GHz)	−100			
$\mathbf{A}^{13C}$ (MHz)	24	1.000	0.000	0.000
	24	0.000	0.9619	0.2588
	212	0.000	−0.2588	0.9619
$\mathbf{A}^{\alpha H}$ (MHz)	−91	1.000	0.000	0.000
	−28	0.000	1.000	0.000
	−63	0.000	0.000	1.000

presently computationally unfeasible. However, general uncertainty estimates for the *g*-values and electron−electron dipolar coupling are 0.01 and 50 MHz, respectively. Uncertainties in the hyperfine coupling values for nuclei, which have been isotopically labeled, are approximately 20 MHz. Note the parameters used in the simulations are reported to a greater precision than can be considered meaningful on the basis of these uncertainty estimates. This is done to demonstrate that parameters which have been previously determined for the individual (noninteracting) paramagnetic species produce simulations consistent with the experimental spectra presented here when incorporated into an electron−electron exchange and dipolar coupled model.

Parameters used in the simulations are given in Table 1. Direction cosines are given with respect to the cob(II)alamin Zeeman principal axis system. **D** is the electron−electron dipolar (zero-field splitting) interaction with principal values $-D/3 + E$, $-D/3 - E$, and $2D/3$. The proton, deuteron, and/or ^{13}C hyperfine coupling parameters used for selected simulations are indicated in the figure captions.

RESULTS AND DISCUSSION

EPR Conditions. The nature of the organic radical(s) formed in catalytically active glutamate mutase was investigated using glutamate substrates that were labeled with either ^{13}C (**1b**−**d**, Scheme 1) or ^{2}H (**1e**−**h**) in a site-specific manner. Each of these glutamates gave an EPR spectrum with the same *g*-value and a shape similar to that of the spectrum from unlabeled glutamate (Figures 1 and 2, respectively). With (2*S*,3*S*)-3-methylaspartate as substrate, a signal was observed that was almost identical to that from unlabeled glutamate (data not shown). Hence, all spectra pertain to complete equilibration of glutamate with 3-methylaspartate ($K_{eq} = 0.093$; Switzer, 1982). The equilibration of the deuterium in the *Si* position of [4,4-$^{2}H_2$]glutamate with the two hydrogens at C-3 via 5′-deoxyadenosine was measured by ^{2}H NMR. This showed two signals at 2.06 ppm (C-3) and at 2.32 ppm (C-4) with relative intesities of ∼ 0.6/1 in the equilibrated glutamate. If only the 4-H_{Si} is abstracted (Sprecher et al., 1966) and in the absence of any isotope effect, a ratio of 0.5 should be obtained, independent of the degree of deuteration at C-4; otherwise the ratio would be >0.5. The exchange of the solvent H_2O by D_2O gave no detectable change of the EPR spectrum obtained with unlabeled glutamate (Figure 3, spectra a and b). Therefore, any influence on the EPR spectra of the solvent could be excluded. This agrees with the observation that during the glutamate mutase reaction no hydrogen transfer via the solvent takes place **(**Switzer, 1982**)**. In another experiment, (*S*)-[^{15}N]glutamate was used as substrate, again giving a spectrum almost identical with that induced by unlabeled (*S*)-glutamate (Figure 3, spectra a and c) and thus excluding the possibility of a nitrogen-based radical. Spectra 2 and 3 in Figure 1A, spectrum 2 in Figure 2A, and spectrum c in Figure 3 show a feature around 290 mT, which is due to the g_{xy} signal of cob(II)alamin present in inactive enzyme. The low intensity of this feature indicates that the eight g_z peaks of this cob(II)alamin species are too small to influence the main signal between 300 and 360 mT.

^{13}C-Labeled Glutamates as Substrates. The EPR spectrum obtained by incubating [4-^{13}C]glutamate (**1d**, Scheme 1) with glutamate mutase indicates that the 4-glutamyl radical (**3d**) is the primary intermediate derived by hydrogen atom abstraction from (**1d**) (Figure 1A,B, spectra 4). The substantial broadening caused by the additional hyperfine coupling to the ^{13}C atom almost obliterated the cobalt hyperfine splittings, proving that C-4 is the main site of unpaired electron density. Comparing the spectrum (Figure 1A, spectrum 2) obtained with [2-^{13}C]glutamate (**1b**) to that of unlabeled glutamate (Figure 1A, spectrum 1) shows that the g'_{xy} and g'_z signals are slightly broadened. This effect was not observed with [3-^{13}C]glutamate (**1c**), with which a spectrum was obtained (Figure 1A, spectrum 3) almost identical to that from unlabeled glutamate. Although the spectral changes are slight, it might be concluded that a radical derived from the substrate labeled at C-2 (**1b**), i.e., the 2-glycinyl radical (**5b**), might be a minor coupling partner for the EPR signals (vide infra). However, this conclusion requires verification. With [4-^{13}C]glutamate (**1d**) as substrate, an additional signal at $g \approx 2.0$ was detected (Figure 1A, spectrum 4). This probably arises from an organic radical of unknown origin contributing approximately only 1% of the spin concentration. It exhibited different power and temperature dependencies from the rest of the spectrum. Thus, at 77 K the signal was absent and a completely smooth spectrum was obtained with an unresolved hyperfine splitting of the g_z line (Figure 1B, spectrum 4).

^{2}H-Labeled Glutamates as Substrates. Incubation of glutamate mutase with perdeuterated glutamate (**1h**, Scheme 1) produced spectrum 5 shown in Figure 2A. The narrowing of the spectral features for the radical(s) derived from **1h** as opposed to unlabeled glutamate (spectrum 1) indicates significant proton hyperfine couplings in the spectrum of the unlabeled radical(s), but the origin of these couplings cannot be delineated from the perdeuterated glutamate. Therefore, EPR spectra were measured using glutamates (**1e**−**g**) specifically deuterated at each carbon from C-2 to C-4 (Figure 2A, spectra 1−4). Only [4,4-$^{2}H_2$]glutamate (**1g**) gave significantly sharper signals in the hyperfine splittings of the g_z line and also for some features in the g_{xy} line (spectrum 4), as observed with perdeuterated glutamate (spectrum 5).

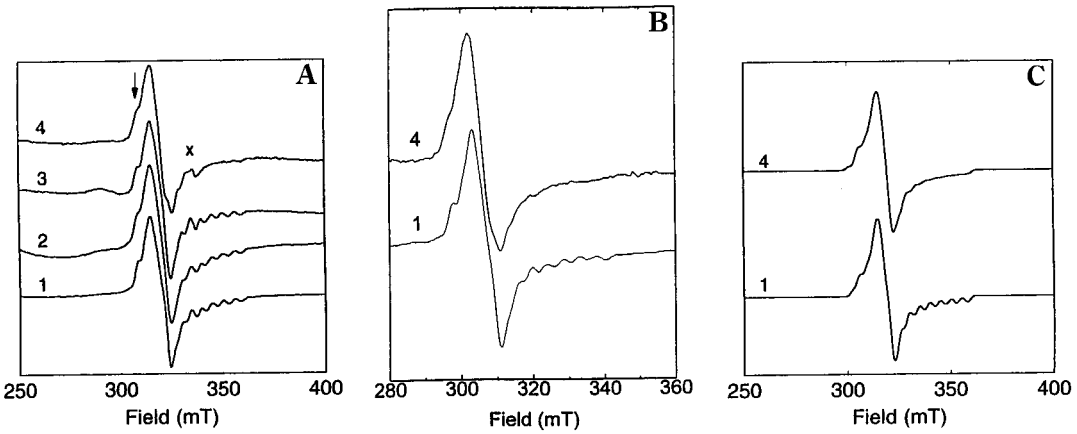

FIGURE 1: (A) Influence of ^{13}C-labeled (*S*)-glutamate species (30 mM each) on the EPR spectra of glutamate mutase (components E + S with an excess of coenzyme B_{12}) at 50 K. Spectrum 1, unlabeled glutamate; spectrum 2, [2-^{13}C]glutamate; spectrum 3, [3-^{13}C]glutamate; spectrum 4, [4-^{13}C]glutamate. The arrow indicates differences of spectra 2 and 4 as compared to spectra 1 and 3. The small signal in spectrum 4 marked with an X is not visible at 77 K as shown in panel B. (C) Simulations corresponding to the experimental spectra 1 and 4 displayed in panels A and B. Spectrum 1: Simulation incorporating one strongly coupled α-proton (hyperfine coupling parameters −91, −28, −63 MHz). Spectrum 4: Simulation parameters used are identical to those for spectrum 1 with the addition of a hyperfine interaction consistent with ^{13}C ($I = {}^1/_2$, hyperfine coupling parameters equal to 24, 24, and 212 MHz); see text for further explanation and for other simulation parameters. For both simulations, unresolved hyperfine splittings from other strongly coupled protons are subsumed in a 2.2 mT Gaussian broadening function.

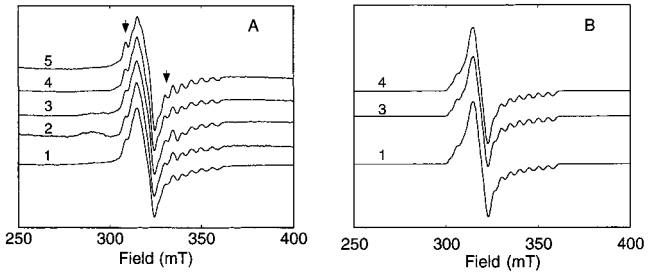

FIGURE 2: (A) Influence of ^{2}H-labeled (*S*)-glutamate species (30 mM each) on the EPR spectra of glutamate mutase (components E + S with an excess of coenzyme B_{12}) at 50 K. Spectrum 1, unlabeled glutamate; spectrum 2, [2-^{2}H]glutamate; spectrum 3, [3,3-$^2H_2$]glutamate; spectrum 4, [4,4-$^2H_2$]glutamate; spectrum 5, [2,3,3,4,4-$^2H_5$]glutamate. The arrows indicate differences of spectra 4 and 5 as compared to spectra 1, 2, and 3. The feature at $g = 2.3$ in spectrum 2 is due to a small amount of cob(II)alamin. (B) Simulations corresponding to experimental spectra displayed in panel A. Spectrum 1: Simulation incorporating one strongly coupled α-proton ($I = {}^1/_2$, hyperfine principal values −91, −28, and −63 MHz). Spectrum 3: Simulated substitution of the α-proton by a deuteron ($I = 1$, hyperfine coupling principal values −14, −4, and −10 MHz). Spectrum 3 is a weighted sum of α-deuteron and α-proton simulations (weights of 0.9 and 0.1, respectively) to reflect the level of glutamate C4 isotopic enrichment. The small amout of deuterium that becomes bound to C3 due to the equilibration of C3 protons and the deuterium at the *Si*-position of C4 is neglected in this simulation. Spectrum 4: Simulation incorporating hyperfine coupling consistent with 2 β-deuterons/protons, both of which form a dihedral angle $\theta = 60°$ with respect to the C4 p-orbital ($A_{iso} = 26$ MHz/4 MHz for each proton/deuteron, respectively). The deuterons bound to C3 are in equilibrium with H_{Si} at C4 (see text). Thus, simulation 4 is the sum of four subspectra corresponding to species deuterated at C3 weighted as follows: two deuterons (weight of 0.45), two protons (0.11), one proton and one deuteron (0.44). For all simulations, unresolved hyperfine splittings from strongly coupled nuclei not explicitly modeled in the simulations are subsumed in a 2.2 mT Gaussian broadening function. See text, Table 1, and Figure 5 for further explanation and for other simulation parameters.

It is of interest that [4,4-$^2H_2$]glutamate exhibits a kinetic isotope effect $^D(V_{max}/K_m) = 6.7 \pm 1.0$ when assayed under standard conditions, whereas [2-^{2}H]glutamate and [3,3-$^2H_2$]-glutamate both showed $^D(V_{max}/K_m) = 1.1 \pm 0.1$ [see also Hartzoulakis and Gani (1994) and Zelder et al. (1994a)]. It may be noted that at the same enzyme concentrations the deuterated glutamates gave EPR spectra of the same intensity as compared to that of unlabeled glutamate (the concentration of spins was up to 50% that of component E). Thus the earlier observed 7-fold lower intensity with perdeuterated glutamate (Zelder et al., 1994a) could not be confirmed. It was probably due to a lower concentration of active enzyme.

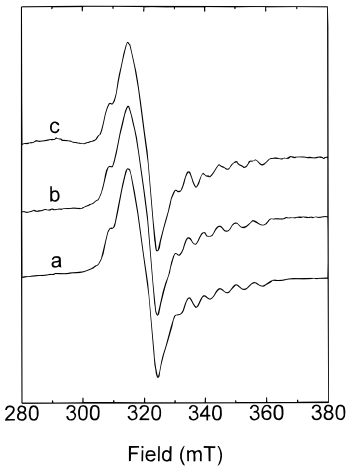

FIGURE 3: EPR spectra of glutamate mutase (components E + S with an excess of coenzyme B_{12}) under different conditions at 50 K. Spectrum a, 30 mM unlabeled (*S*)-glutamate; spectrum b, as spectrum a but in D_2O; spectrum c, 30 mM (*S*)-[^{15}N]glutamate. For experimental details see Materials and Methods.

The most straightforward explanation for the results described is the dominant participation of the substrate-derived radical (**3a**) in an exchange-coupled pair with cob(II)alamin, as deduced from the data for ^{13}C labeling. If the glycinyl radical (**5a**) were a dominant species, then deuterium substitution at C-2 of glutamate should substantially narrow the EPR spectrum, with substitution at C-3 and C-4 having minimal effects, in contrast to what was observed. The site-specific deuteration data at C-3 also exclude a significant contribution by the methyleneaspartate radical (**4a**), in agreement with the data from ^{13}C labeling.

Scheme 2: Postulated Arrangement of Cob(II)alamin, 5′-Deoxyadenosine (Ado-CH_3), and the 4-Glutamyl Radical (**3a**) following Abstraction of H_{Si} from (*S*)-Glutamate (**1a**) by the 5′-Deoxyadenosyl Radical ($AdoCH_2$•) Derived from Coenzyme B_{12}

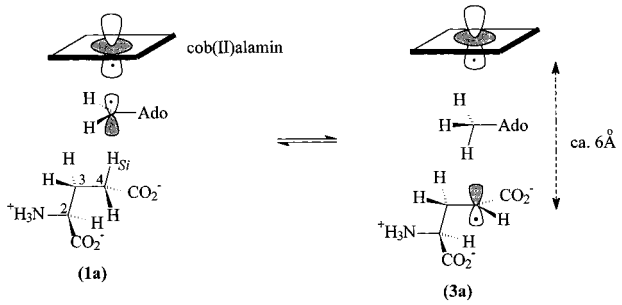

Simulations of the EPR Spectra. The major characteristics of the EPR spectrum of catalytically active glutamate mutase are similar to those of the ribonucleotide reductase of *L. leichmannii* (Gerfen et al., 1996). These similarities include the apparent *g* value of ~2.1 and a resolved cobalt hyperfine splitting of 5.0 mT. With ribonucleotide reductase, the spectral characteristics can be reproduced using a model of cob(II)alamin interacting via exchange and dipolar couplings with an organic radical. Simulation of the spectrum for glutamate mutase with unlabeled glutamate used the parameters presented in Table 1. The simulated spectra (Figures 1C and 2B) with principal *g* values < 2.007 for the radical partner of cob(II)alamin is in good agreement with the observed spectrum, while larger *g* values (up to 2.015) gave a poorer fit. The lower limit for the exchange coupling determined in this study ($|J_{ex}|$ > 4 GHz) indicates an interaction (either direct or indirect) of the molecular orbitals containing the electron spins and suggests that the cob(II)alamin is close to the organic radical. This proximity is supported by the size of the dipolar coupling needed to reproduce the spectral width, which gives an interspin distance of $r = 6.6 \pm 0.9$ Å. The model shown in Scheme 2 in which 5′-deoxyadenosine serves to insulate the 4-glutamyl radical (**3a**) from cob(II)alamin is consistent with this finding.

An approximate lower limit for the value of $|J_{ex}|$ was established by comparing simulations with experimental spectra in a manner similar to that described previously (Gerfen et al., 1996). For values of $|J_{ex}|$ < 4 GHz, the spectral features associated with the organic radical and the cob(II)alamin do not fully "coalesce" at the proper magnetic field value. In addition, for $|J_{ex}|$ < 4, spectral features split upfield and downfield (by values corresponding to $|J_{ex}|$) from the main central peaks are clearly discernible in the simulations but not in the experimental spectra. These transitions, which involve what becomes the singlet electronic state in the high $|J_{ex}|$ limit, become less intense with increasing $|J_{ex}|$. Simulations indicate that when $|J_{ex}|$ > 4 GHz these transitions are too weak to detect experimentally. This observation is used as the criterion to establish the estimate for the lower limit of $|J_{ex}|$. Variation of $|J_{ex}|$ below approximately 15 GHz influenced the simulations in the 300−350 mT range; the simulations were relatively insensitive to exchange couplings above that value, and thus a value of $|J_{ex}| = 100$ GHz was used in all simulations. However, use of this value does not constitute an assignment of the exchange coupling beyond the fact that it is larger than the estimated lower limit of 4 GHz. Previous temperature-dependent EPR studies of the adenosylcobalamin-dependent enzyme ribonucleoside triphosphate reductase suggest that the exchange-coupled species in that system has a singlet ground state (Licht et al., 1996). By analogy, the sign of J_{ex} is taken to be negative for glutamate mutase. Additional frequency- and temperature-dependent experiments must be performed in order to determine the sign and further refine the magnitude of J_{ex} in the glutamate mutase system.

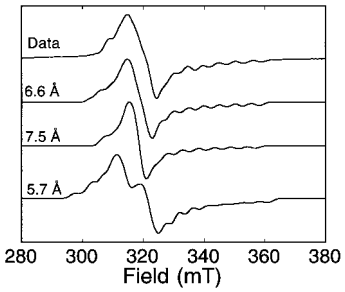

FIGURE 4: Determination of the uncertainty estimate for the electron−electron interspin distance. The experimental spectrum is the same as in Figures 1A and 2A, spectra 1. In the simulated spectra the distance *r* between cob(II)alamin and the organic radical (as indicated on each spectrum) was varied. Simulation was performed as described in the legend of Figure 2 using following electron−electron dipolar coupling parameters $D = 300$ MHz for $r = 6.6$ Å, 200 MHz for 7.5 Å, and 466 MHz for 5.7 Å.

The estimate for the distance between the two electron spins has been obtained from the size of electron−electron dipolar interaction *D*. Caution must be exercised in making this estimate, since it approximates the two electron spins as point dipoles and neglects the possible contribution from anisotropic exchange interactions. Nonetheless, this analysis has been used successfully in similar systems [Cu(II)−Cu(II) and Cu(II)−nitroxide] (Eaton & Eaton, 1989) and thus is employed here. More extensive analysis of structural implications of both electron−electron dipolar and exchange interactions have been carried out (Coffman & Buettner, 1979a,b). Making the approximation (Wertz & Bolton, 1986; Eaton & Eaton, 1989) that $2D/3 = \mu_o g_a g_b \beta_e^2/4\pi h r^3$ with β = Bohr magneton, h = Planck's constant, μ_o= vacuum permeability, g_a= 2.0, g_b= 2.2, and $D = 300$ MHz gives $r = 6.6$ Å. Figure 4 shows simulations incorporating this value of *D* as well as values that lie above and below the range which give reasonable fits to the data (corresponding to $r = 5.7$ and 7.5 Å, respectively). From these simulations an estimate to the uncertainty in the interspin distance of ± 0.9 Å is obtained.

Simulations of the EPR spectra from the isotopically labeled substrates (**1b**−**1h**) with parameters given in Table 1 confirmed that the spectral effects were consistent with the structures proposed for the radicals. The simulations for the glutamate radicals deuterated at C-3 and C-4 are shown in Figure 5. The 4-glutamyl species (**3a**) has a total of three protons in an α or β position to the radical center. The magnitude of the hyperfine couplings to H_α and H_β in a p-type organic radical (see structures **7a** and **7b**) depends

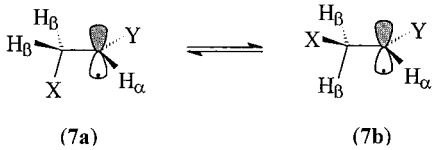

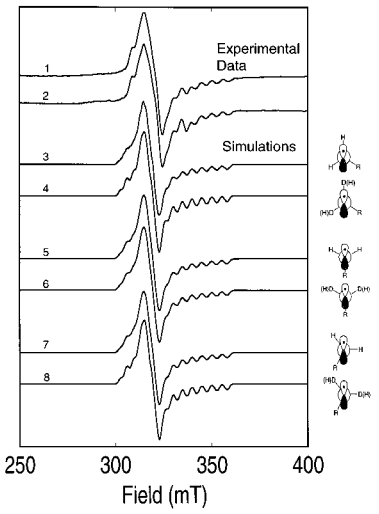

FIGURE 5: Spectroscopic evidence for the geometry of the 4-glutamyl radical as depicted in structure **3a** based on deuteration at the glutamate C3 position. Spectrum 1, experimental with unlabeled glutamate. Spectrum 2, experimental with [3,3-$^2H_2$]-glutamate. Spectra 3−8 were simulated incorporating isotropic hyperfine coupling parameters consistent with varying dihedral angles for two hydrogens adjacent to a carbon-centered radical with $\rho = 0.8$. (eq 1). The deuterons bound to C3 are in equilibrium with H_{Si} at C4. Thus the simulations 4, 6, and 8 are the sum of four subspectra corresponding to species deuterated at C3 weighted as follows: two deuterons (weight of 0.45), two protons (0.11), one proton and one deuteron (0.22 each position). In spectra 3 and 4 the angles for the β-protons/deuterons were $\theta = 0°$ ($A_{iso} = 96$ MHz/15 MHZ) and $\theta = 60°$ ($A_{iso} = 26$ MHz/4 MHz) with a Gaussian broadening of 1.2 mT. For spectra 5 and 6, $\theta = 60°$ was the same for both β-protons/deuterons ($A_{iso} = 26$ MHz/4 MHz) and a Gaussian broadening of 2.5 mT was used. For spectra 7 and 8 the angles were $\theta = 30°$ ($A_{iso} = 72$ MHz/11 MHZ) and $\theta = 90°$ ($A_{iso} = 2$ MHz/0 MHz), and a Gaussian broadening of 1.9 mT was used. The simulation pair (spectra 5 and 6) that best matches the experimental data (spectra 1 and 2) corresponds to the radical geometry in which R eclipses the *p*-orbital at C-4 (structures **3a** and **7a**) consistent with two β-protons at approximately $\theta = 60°$.

on the molecular and electronic structure of the species, but both can be substantial (<2 mT for a proton, reduced to < 0.35 mT for deuterium) (Wertz & Bolton, 1986). The hyperconjugative effects from H_β protons in a radical of type **7** show a strong angular dependence. Deuteration at C-4 shows a much greater narrowing effect than deuteration at C-3, although the effect is less than the narrowing observed in the signal induced by perdeuterated glutamate (**1h**), where 1.0 $^2H_\alpha$ and 2.0 $^2H_\beta$ rather than 0.8−0.9 $^2H_\alpha$ and 0.6−0.7 $^2H_\beta$ interact with the radical. These values were calculated for glutamate with 90% ^2H at C-4 and a ^2H enrichment at C-3 during equilibration; see ^2H NMR data and Materials and Methods. Simulations incorporating typical couplings for $^1H_\alpha$ ($^2H_\alpha$) and $^1H_\beta$ ($^2H_\beta$) in structures of type **3** and **4** were consistent with the degree of narrowing observed in the experimental spectra.

In the fragmentation−recombination mechanism proposed for glutamate mutase (Beatrix et al., 1995), a specific conformation is required for the 4-glutamyl radical (**3a**) (as shown in Scheme 1) to permit a stereoelectronically allowed fission to acrylate (**6**) and the 2-glycinyl radical (**5a**). It may be assumed that the conformation of the protein-bound radical corresponds closely to that needed for fission. The geometry of the 4-glutamyl radical species was investigated by examining the C-3 proton hyperfine interactions (Figure 5). These β-protons experience a mainly isotropic hyperfine interaction that is described by

$$A_{iso}^{\beta} = \rho(A + B\cos^2\theta) \quad (1)$$

in which ρ is the spin density on the carbon atom adjacent to the methylene group, A and B are constants whose values depend on structural details of the radical, and θ is the angle defined by the methylene C−H bond and p-orbital axis. To estimate the values of θ for the two C-3 protons, we take the empirically determined values for A and B (92 μT and 4.26 mT, respectively) and use a spin density value on C-4 of 0.8 as determined by Ballinger et al. (1992) for a similar radical species. This analysis is approximate since the β-proton hyperfine couplings are manifest in the spectra only as broadening. However, simulations in which one C-3 proton eclipses the C-4 p-orbital (giving θ values of 0° and 60° for the β-protons) yields a degree of spectral narrowing upon C-4 deuteration which is much greater than that observed experimentally. A molecular orientation giving $\theta = 60°$ for both C-3 protons (i.e., the minimum for the sum of the hyperfine couplings, in which the glycinyl group R eclipses the C-4 p-orbital) gives best fits to the experimental spectra. Simulations for which the position of the glycinyl group (R) relative to the *p*-orbital of the radical deviates more than 30° away from this R-eclipsed conformation yield a degree of narrowing which is larger than that obtained in the experimental data. The eclipsed orientation is proposed to be necessary for the fission of the bond from C-3 to the glycinyl moiety in the fragmentation mechanism shown in Scheme 1. It is concluded that the isotopic labeling experiments and their simulations favor the 4-glutamyl radical (**3a**) as the major coupling partner of cob(II)alamin.

*Do Other Species besides the Substrate-Derived Radical (**3a**) Contribute to the EPR Spectra?* The question arises as to whether the EPR spectra represent an interaction of more than one organic radical with cob(II)alamin, with the 4-glutamyl radical (**3a**) being the most prominent species. With the possible exception of [3-^{13}C]glutamate (**1c**), none of the other ^{13}C-labeled or deuterated glutamates induced an EPR signal that was identical to the spectrum derived from unlabeled (*S*)-glutamate. Deuteration at C-2 leads to a spectrum with slightly sharper features than the spectrum induced by unlabeled glutamate, while ^{13}C-labeling at C-2 broadens the spectrum (see Figures 1 and 2). These substitutions are not expected to affect a radical center at C-4 and may be taken as evidence for a minor involvement of the 2-glycinyl radical [**5a**; see also Yu et al. (1995)], although the observed narrowing or broadening is rather small. However, the ^{13}C-labeling and deuteration experiments do not show the intermediacy of the 3-methyleneaspartate radical (**4a**), which is probably present in lowest concentration among the radicals **3a**, **4a**, and **5a**.

The large number of parameters required for the simulation of these spectra preclude the possibility of a rigorously unique fit given the present data. Several experimental strategies exist that may provide additional refinements on parameters associated with both the electon−electron and the electron−nuclear interactions. These strategies include the acquisition of spectra at different EPR frequencies (Buettner & Coffman, 1977; Eaton & Eaton, 1989; Gerfen et al., 1996), the observation of half-field transitions (Eaton

& Eaton, 1989), and electron spin−echo envelope modulation (ESEEM) and electron nuclear double resonance (ENDOR) spectroscopies (Hoff, 1989). In addition, computational methods developed to quantitatively fit dipolar coupled ^{15}N-labeled dinitroxide systems may be extended to the more complicated cob(II)alamin radical systems (Hustedt et al., 1997). These experimental and computational strategies are presently being explored. However, the results of the experiments incorporating site-specific isotopically labeled glutamate combined with the present spectral simulations strongly support the following conclusions: (1) the EPR spectra arise from cob(II)alamin interacting with an organic radical species, (2) the predominant radical species is a substrate-derived 4-glutamyl radical, (3) the electron spins experience an exchange coupling ($|J_{ex}| > 4$ GHz) and are estimated to be 6.6 Å apart, and (4) the structure of the radical is such that the C3−C2 bond approximately eclipses the C4 p-orbital.

Other Coenzyme B_{12}-Dependent Enzymes. The family of carbon skeleton rearranging enzymes dependent on B_{12} coenzyme consists of glutamate mutase, 2-methyleneglutarate mutase, methylmalonyl-CoA mutase, and isobutyryl-CoA mutase [for recent reviews see Banerjee (1997) and Golding and Buckel (1997)]. It is widely accepted that the minimal mechanism for these enzymes requires a substrate-derived radical (Halpern, 1985; Stubbe, 1989; Frey, 1990; Finke, 1990). It has been proposed that all of these enzymes follow a similar fragmentation−recombination mechanism (Buckel & Golding, 1996). If this is true, then it is likely that the EPR spectra from 2-methyleneglutarate mutase (Beatrix et al., 1995) and methylmalonyl CoA mutase (Zhao et al., 1992, 1994; Padmakumar & Banerjee, 1995) also represent the interaction of cob(II)alamin with the substrate-derived radical. It was previously stated that EPR spectra for methylmalonyl-CoA mutase were not modified by ^{13}C labeling of the substrate (Zhao et al., 1994). However, the label was in the methyl group of methylmalonyl-CoA and would be expected to have the same insignificant effect as observed with [3-^{13}C]glutamate and glutamate mutase (Figure 1A, spectra 1 and 3), from which we concluded that the 3-methyleneaspartate radical did not contribute to the EPR signals. From our results one can predict that the 3-succinyl-CoA radical rather than the methylenemalonyl-CoA radical would be the predominant EPR-active species in the reaction catalyzed by methylmalonyl-CoA mutase. For isobutyryl-CoA mutase (Brendelberger et al., 1988; Moore et al., 1995), no EPR signals have been reported, but it will be interesting to determine if this enzyme−substrate system will exhibit spectra similar to those observed with the other carbon skeleton rearranging enzymes.

Although there are gross similarities between the spectra from glutamate mutase and the ribonucleotide triphoshate reductase of *Lactobacillus leichmannii*, significant differences exist, particularly with regard to the spectral position of the cobalt hyperfine structure. Simulations indicate that this difference can be attributed to the characteristics of the organic radical involved in the exchange-coupled pair. For ribonucleotide reductase, g values of 2.2, 2.0, and 1.99 consistent with a thiyl radical were required to produce reasonable fits, whereas for glutamate mutase g values consistent with a carbon-centered radical were necessary.

Comparison with the Substrate-Derived Radical from Lysine 2,3-Aminomutase. The proposed structure for the major radical interacting with cob(II)alamin in glutamate mutase is the substrate-derived species **3a**. This has its electron spin density primarily located in a carbon π-orbital α to a carboxylate group. It is interesting to note that the same type of substrate-derived radical was observed with lysine 2,3-aminomutase (Ballinger et al., 1992), which catalyzes the intramolecular shift of the α-amino group of lysine to the β-position concomitant with an intermolecular H-migration in the reverse direction. Although this reaction is closely related to coenzyme B_{12}-dependent carbon skeleton rearrangements, this enzyme is cobalamin-independent. Hence, the absence of interfering electron−electron interactions with cob(II)alamin allowed the accurate determination of the radical species hyperfine coupling parameters using isotopic substitution, resolution enhancement techniques (Ballinger et al., 1992), and electron spin−echo envelope modulation (ESEEM) spectroscopy (Ballinger et al., 1995). The parameters for both the proton and ^{13}C hyperfine values used in simulations for the substrate-derived radical in the present study were consistent with those determined for the radical observed under steady-state conditions during catalysis of lysine 2,3-aminomutase.

Conclusions. It had been suggested 38 years ago that substrate-derived radicals are involved in the catalysis of carbon skeleton rearranging mutases (Eggerer et al., 1960). The identification of the 4-glutamyl radical now confirms this old hypothesis. A fragmentation−recombination mechanism (Scheme 1) has been proposed for coenzyme B_{12}-dependent glutamate mutase (Beatrix et al., 1995; Buckel & Golding, 1996). This mechanism involves the equilibration of radicals **3a** and **4a** via the 2-glycinyl radical (**5a**) and acrylate (**6**). The results presented in this paper provide strong support for the postulated intermediacy of the 4-glutamyl radical (**3a**), which is shown to be interacting with ("talking to") cob(II)alamin at a distance of about 6.6 Å. Tentative support for the participation of the 2-glycinyl radical (**5a**) in the catalytic cycle was also obtained. Further confirmation of this assignment is required before the intermediacy of radical **5a** and its partner acrylate in the glutamate mutase reaction can be accepted.

ACKNOWLEDGMENT

We thank Christopher H. Edwards (Department of Chemistry, University of Newcastle upon Tyne) for performing initial steps of the synthesis of [4-^{13}C]glutamate, Iris Schall (Laboratorium für Mikrobiologie, Philipps-Universität Marburg) for preparing β-methylaspartase from *Clostridium tetanomorphum*, which is required for the spectrophotometric assay of glutamate mutase, and Professor Stefan Berger (Fachbereich Chemie, Philipps-Universität Marburg) for measuring and interpreting the NMR spectra. We also would like to quote Professor Brian M. Hoffman (Northwestern University, Evanston, IL) who exclaimed upon seeing our EPR spectra, "That's clear, there are two radicals talking to each other!"

REFERENCES

Abeles, R. H., & Dolphin, D. (1976) *Acc. Chem. Res. 9*, 114−120.
Babior, B. M. (1988) *Bio Factors 1*, 21−26.

Ballinger, M. D., Frey, P. A., & Reed, G. H. (1992) *Biochemistry 31*, 10782−10789.
Ballinger, M. D., Frey, P. A., Reed, G. H., & LoBrutto, R. (1995) *Biochemistry 34*, 10086−10093.
Banerjee, R. (1997) *Chem. Biol. 4*, 175−186.
Barker, H. A., Rooze, V., Suzuki, F., & Iodice, A. A. (1964) *J. Biol. Chem. 239*, 3260−3266.
Beatrix, B., Zelder, O., Kroll, F., Örlygsson, G., Golding, B. T., & Buckel, W. (1995) *Angew. Chem. 107*, 2573−2576; *Angew. Chem., Int. Ed. Engl. 34*, 2398−2401.
Brendelberger, G., Rétey, J., Ashworth, D. M., Reynolds, K., Willenbrock, F., & Robinson, J. A. (1988) *Angew. Chem. 100*, 1122−1124; *Angew. Chem., Int. Ed. Engl. 27*, 1089−1090.
Buckel, W. (1980) *Arch. Microbiol. 127*, 167−169.
Buckel, W., & Barker, H. A. (1974) *J. Bacteriol. 117*, 1248−1260.
Buckel, W., & Golding, B. T. (1996) *Chem. Soc. Rev. 26*, 329−337.
Buettner, G. R., & Coffman, R. E. (1977) *Biochim. Biophys. Acta 480*, 495−505.
Coffman, R. E., & Buettner, G. R. (1979a) *J. Phys. Chem. 83*, 2387−2392.
Coffman, R. E., & Buettner, G. R. (1979b) *J. Phys. Chem. 83*, 2392−2400.
Eaton, G. R., & Eaton, S. S. (1989) in *Biological Magnetic Resonance* (Berliner, L. J., & Reuben, J., Eds.) Vol. 8, pp 339−397, Plenum, New York.
Eggerer, H., Stadtman, E. R., Overath, P., & Lynen, F. (1960) *Biochem. Z. 333*, 1−9.
Golding, B. T., & Buckel, W. (1997) in *Comprehensive Biological Catalysis* (Sinnott, M. L., Ed.) Academic Press, London (in press).
Finke, R. (1990) in *Molecular Mechanisms in Bioorganic Processes* (Bleasdale, C., & Golding, B. T., Eds.) pp 244−280, Royal Society of Chemistry, Cambridge, U.K.
Frey, P. A. (1990) *Chem. Rev. 90*, 1343−1357.
Gerfen, G. J., Licht, S., Willems, J.-P., Hoffmann, B. M., & Stubbe, J. (1996) *J. Am. Chem. Soc. 118*, 8192−8197.
Golding, B. T. (1982) in B_{12} (Dolphin, D., Ed.) Vol. 1, pp 543−582, Wiley, New York.
Golding, B. T., & Radom, L. (1976) *J. Am. Chem. Soc. 92*, 6331−6338.
Halpern, J. (1985) *Science 227*, 869−875.
Hartrampf, G., & Buckel, W. (1984) *FEBS Lett. 171*, 73−78.
Hartzoulakis, B., & Gani, D. (1994) *Proc. Ind. Acad. Sci. (Chem. Sci.) 106*, 1165−1176.
Hoff, A. J. (1989) *Advanced EPR: Applications in Biology and Biochemistry*, Elsevier, Amsterdam.
Hustedt, E. J., Smirnov, A. I., Laub, C. F., Cobb, C. E., & Beth, A. H. (1997) *Biophys. J. 74*, 1861−1877.
Leutbecher, U., Albracht, S. P. J., & Buckel, W. (1992) *FEBS Lett. 307*, 144−146.
Licht, S., Gerfen, G. J., & Stubbe, J. (1996) *Science 271*, 477−481.
Luschinsky Drennan, C., Huang, S., Drummond, J. T., Matthews, R. G., & Ludwig, M. L. (1994) *Science 266*, 1669−1674.
Michel, C., Albracht, S. P. J., & Buckel, W. (1992) *Eur. J. Biochem. 205*, 767−773.
Moore, B. S., Eisenberg, R., Weber, C., Bridges, A., Nanz, D., & Robinson, J. A. (1995) *J. Am. Chem. Soc. 117*, 11285−11291.
Murray III, A., & Williams, D. L. (1958) *Organic syntheses with isotopes, part II: Organic compounds labeled with isotopes of the halogens, hydrogen, nitrogen, oxygen, phosphorus, and sulfur*, pp 1301−1302 Interscience Publishers, New York and London.
Orme-Johnson, W. H., Beinert, H., & Blakely, R. L. (1974) *J. Biol. Chem. 249*, 2338−2343.
Padmakumar, Ru., & Banerjee, R. (1995) *J. Biol. Chem. 270*, 9295−9300.
Padmakumar, Ru., Taoka, S., Padmakumar, Ra., & Banerjee, R. (1995) *J. Am. Chem. Soc. 117*, 7033−7034.
Pilbrow, J. R. (1982) in B_{12} (Dolphin, D., Ed.) Vol. 1, pp 431−462, Wiley, New York.
Rétey, J. (1982) in B_{12} (Dolphin, D., Ed.) Vol. 2, pp 357−380, Wiley, New York.
Rose, Z. B. (1984) *J. Biol. Chem. 235*, 928−933.
Sprecher, M., Switzer, R. L., & Sprinson, D. B. (1966) *J. Biol. Chem. 241*, 864−871.
Stubbe, J. A. (1989) *Annu. Rev. Biochem. 58*, 257−285.
Stupperich, E., Eisinger, H. J., & Albracht, S. P. J. (1990) *Eur. J. Biochem. 193*, 105−109
Switzer, R. L. (1982) in B_{12} (Dolphin, D., Ed.) Vol. 2, pp 357−380, Wiley, New York.
Villieras, J., & Rambaud, M. (1982) *Synthesis* 924−926.
Wertz, J. E., & Bolton, J. R., (1986) *Electron Spin Resonance. Elementary Theory and Practical Applications*, Chapman and Hall, New York.
Yu, D., Rauk, A., & Armstrong, D. A. (1995) *J. Am. Chem. Soc. 117*, 1789−1796.
Zelder, O., & Buckel, W. (1993) *Biol. Chem. Hoppe-Seyler 374*, 85−90.
Zelder, O., Beatrix, B., Leutbecher, U., & Buckel, W. (1994a) *Eur. J. Biochem. 226*, 577−585.
Zelder, O., Beatrix, B., & Buckel, W. (1994b) *FEMS Microbiol. Lett. 118*, 15−22.
Zelder, O., Beatrix, B., Kroll, F., & Buckel, W. (1995) *FEBS Lett. 369*, 252−254.
Zhao, Y., Such, P., & Rétey, J. (1992) *Angew. Chem. 104*, 212−213; *Angew. Chem., Int. Ed. Engl. 31*, 215−216.
Zhao, Y., Abend, A., Kunz, M., Such, P., & Rétey, J. (1994) *Eur. J. Biochem. 225*, 891−896.

BI971393Q